Article

Bifurcation analysis and chaos control in a discrete-time predator-prey system with Crowley-Martin functional response

S. M. Sohel Rana
University of Dhaka, Dhaka-1000, Bangladesh
E-mail: srana.mthdu@gmail.com

Received 29 December 2018; *Accepted 5 February 2019*; *Published 1 June 2019*

Abstract

In this paper, the dynamics of a discrete-time predator-prey system with Crowley-Martin functional response is examined. Via application of the center manifold theorem and bifurcation theorems, we algebraically show that the system undergoes a bifurcation (flip or Neimark-Sacker) in the interior of $\mathbb{R}^2_+$. Numerical simulations are presented not only to validate analytical results but also to reveal new dynamical behaviors which include bifurcations, phase portraits, period- 5, 6, 7, 10, 11, 15, 16, 17, 21, 28, and period- 51 orbits, invariant closed cycle, sudden disappearance of chaotic dynamics and abrupt emergence of chaos, and attracting chaotic sets. Furthermore, maximum Lyapunov exponents and fractal dimension are computed numerically to justify the chaotic behaviors of the system. Finally, we apply a strategy of feedback control to control chaos exists in the system.

Keywords predator-prey system with Crowley-Martin functional response; bifurcations; chaos; Lyapunov exponents; feedback control.

Computational Ecology and Software
ISSN 2220-721X
URL: http://www.iaees.org/publications/journals/ces/online-version.asp
RSS: http://www.iaees.org/publications/journals/ces/rss.xml
E-mail: ces@iaees.org
Editor-in-Chief: WenJun Zhang
Publisher: International Academy of Ecology and Environmental Sciences

1 Introduction

Predator-prey interactions have long been studied and have become one of the dominant themes in both biology and mathematical biology due to their universal existence and importance, such as resource-consumer, plant-herbivore, and phytoplankton-zooplankton forms. In recent decades, mathematical models have been established to analyze various complex dynamics of the predator-prey systems in various circumstances. The research on the Crowley-Martin functional response has now drawn great attention (Dong et al., 2015; Li et al., 2015; Tripathi et al., 2016).

Despite plenty and extensive results on dynamics of continuous predator-prey system, studies on discrete predator-prey model are relatively rare. In fact discrete predator-prey model is not a simple parallel promotion of continuous system. Sometimes it shows richer and more complex dynamics than the corresponding continuous model. Besides, for insects with non-overlapping generations, predator-prey system can be

modeled in a discrete-time form; and numerical computation also requires to discretize a continuous-time model (He and Lai, 2011; Elhassanein, 2014; He and Li, 2014; Nedorezov and Neklyudova, 2014; Rana, 2015a-d, 2017, 2019; Zhao et al., 2016; Zhao et al., 2017). These researches have mainly focused on Gauss-type predator-prey interaction with monotonic functional responses. They obtained many complex properties in discrete-time models including the possibility of bifurcations (flip and Neimark-Sacker) and chaos phenomenon which had been derived either by using numerical simulations or by using center manifold theory.

In recent times, a few number of articles in literature discussed the dynamics of discrete-time predator-prey systems with Crowley-Martin functional response (Ren et al., 2017; Zhang et al., 2018). For example, a discrete-time predator-prey system of Leslie type with Crowley-Martin functional response was investigated in Ren et al. (2017), and a discrete predator-prey system with Crowley-Martin Type functional response was studied in Zhang et al. (2018). In their studies, the authors paid their attention to drive the existence of flip and Neimark-Sacker bifurcations by using center manifold theory. In this paper, we consider the following predator-prey system with Crowley-Martin functional response (Crowley and Martin, 1989):

$$\begin{aligned} \dot{x} &= rx\left(1-\frac{x}{K}\right)-\frac{axy}{(1+\alpha x)(1+\beta y)} \\ \dot{y} &= \frac{bxy}{(1+\alpha x)(1+\beta y)}-dy \end{aligned} \tag{1}$$

where x and y stand densities of prey and predator, respectively; r, K, a, b, d, α and β are all positive constants, and $\frac{axy}{(1+\alpha x)(1+\beta y)}$ denotes Crowley-Martin functional response. The parameter r is the intrinsic growth rate of the prey, the parameter K is the carring capacity of the prey and the parameter d is the mortality rate of the predator; a and $\frac{b}{a}$ stand for the effect of capture rate and conversion factor denoting the newly born predators for each captured prey; the parameters α and β are the saturating parameters of Crowley-Martin functional response, α measures the magnitude of interference among prey, and β expresses the interference among the predators.

Forward Euler scheme is applied to system (2) to get the following discrete system

$$\begin{pmatrix} x \\ y \end{pmatrix} \mapsto \begin{pmatrix} x+\delta x\left[r\left(1-\frac{x}{K}\right)-\frac{ay}{(1+\alpha x)(1+\beta y)}\right] \\ y+\delta y\left[\frac{bx}{(1+\alpha x)(1+\beta y)}-d\right] \end{pmatrix} \tag{2}$$

where δ is the step size. The objective is to study systematically the existence condition of a bifurcation (flip or NS bifurcation) in the interior of $\mathbb{R}^2_+$ using bifurcation theory and center manifold theory (Kuzenetsov, 1998; Winggins, 2003).

This paper is organized as follows. Section 2 deals the existence condition for fixed points of system (2) and their stability criterion. In Section 3, we prove that under certain parametric condition system (2) admits a bifurcation. In Section 4, we implement numerical simulations of the system for one or more control parameters which include diagrams of bifurcation, phase portraits, maximum Lyapunov exponents and Fractal dimensions. In Section 5, we use the method of feedback control to stabilize chaos at an unstable trajectories. Finally we carry out a short discussion in Section 6.

2 Fixed Points: Existence and Their Stability

The fixed points of system (2) are solution of

$$\begin{cases} x + \delta x\left[r\left(1-\frac{x}{K}\right) - \frac{ay}{(1+\alpha x)(1+\beta y)}\right] &= x \\ y + \delta y\left[\frac{bx}{(1+\alpha x)(1+\beta y)} - d\right] &= y \end{cases} \tag{3}$$

A simple algebraic computation shows that system (2) has a predator free fixed point $E_1(K,0)$ for all parameter values. Next, it is of great interest to find the positive fixed point of system (2). Suppose that $E_2(x^*,y^*)$ is a positive fixed point of system (2). Then, x^* and y^* are solutions of

$$\begin{cases} r(1-\frac{x^*}{K}) &= \frac{ay^*}{(1+\alpha x^*)(1+\beta y^*)} \\ \frac{by^*}{(1+\alpha x^*)(1+\beta y^*)} &= d \end{cases} \tag{4}$$

From (4), we can see that $x^* \in (0,K)$ is the root of the following cubic equation

$$p_0 w^3 + 3p_1 w^2 + 3p_2 w + p_3 = 0, (p_0 \neq 0), \tag{5}$$

with coefficients $p_0 = \frac{br\alpha\beta}{K}, 3p_1 = \frac{br(1-K\alpha)\beta}{K}, 3p_2 = a(b-d\alpha) - br\beta, p_3 = -ad.$

Now, the transformation $z = p_0 w + p_1$ converts the equation (5) to $z^3 + 3Hz + G = 0$, where$G = {p_0}^2 p_3 - 3p_0 p_1 p_2 + 2{p_1}^3$, $H = p_0 p_2 - {p_1}^2$. Using Cardano's method, we get following result.

Lemma 2.1 *If* $G^2 + 4H^3 > 0$, *then a unique positive fixed point* $E_2(x^*,y^*)$ *of system (2) exists, where* $x^* = \frac{1}{p_0}(q - \frac{H}{q} - p_1)$, $y^* = \frac{-d+bx^*-d\alpha x^*}{d(1+\alpha x^*)\beta}andq$ denotes one of the three values of $\left[\frac{-G+\sqrt{G^2+4H^3}}{2}\right]^{\frac{1}{3}}$.

Next, we investigate stability of system (2) at fixed points. Note that the magnitude of eigenvalues of Jacobian matrix evaluated at fixed point $E(x,y)$ determines the local stability of that fixed point. The Jacobian matrix of system (2) evaluated at fixed point $E(x,y)$ is given by

$$J(x,y) = \begin{pmatrix} a_{11} & a_{12} \\ a_{21} & a_{22} \end{pmatrix} \tag{6}$$

where

$$\begin{aligned} a_{11} &= 1 + \frac{r\delta(K-2x)}{K} - \frac{a\delta y}{(1+\alpha x)^2(1+\beta y)}, \\ a_{12} &= -\frac{a\delta x}{(1+\alpha x)(1+\beta y)^2} \\ a_{21} &= \frac{b\delta y}{(1+\alpha x)^2(1+\beta y)}, \\ a_{22} &= 1 - \frac{\delta(-bx+d(1+\alpha x)(1+\beta y)^2)}{(1+\alpha x)(1+\beta y)^2}. \end{aligned} \tag{7}$$

The characteristic equation of matrix J is

$$\lambda^2 + p(x,y)\lambda + q(x,y) = 0 \tag{8}$$

where $p(x,y) = -trJ = -(a_{11} + a_{22})$ and $detJ = a_{11}a_{22} - a_{12}a_{21}$.

Using Jury's criterion (Elaydi, 1996), we state the following stability conditions of fixed points.

Proposition 2.2 *The predator free fixed point* $E_1(K,0)$ *is a sink if* $0 < \delta < min\left\{\frac{2}{r}, \frac{2(1+K\alpha)}{d+K(\alpha d-b)}\right\}$, *source if* $\delta > min\left\{\frac{2}{r}, \frac{2(1+K\alpha)}{d+K(\alpha d-b)}\right\}$ *and non-hyperbolic if* $\delta = \frac{2}{r}$ *or* $\frac{2(1+K\alpha)}{d+K(\alpha d-b)}$.

It is obvious that when $\delta = \frac{2}{r}$ or $\frac{2(1+K\alpha)}{d+K(\alpha d-b)}$, the two eigenvalues of $J(E_1)$ are $\lambda_1 = 1 - r\delta$ and $\lambda_2 = 1 - \alpha d + \frac{bK\delta}{1+K\alpha}$. Therefore, a flip bifurcation can occur if parameters change in small vicinity of $FB^1_{E_1}$ or $FB^2_{E_1}$:

$$FB^1_{E_1} = \left\{(r,K,a,b,d,\alpha\beta,\delta) \in (0,+\infty): \delta = \frac{2}{r}, \delta \neq \frac{2(1+K\alpha)}{d+K(\alpha d-b)}\right\}$$

or

$$FB^2_{E_1} = \left\{(r,K,a,b,d,\alpha\beta,\delta) \in (0,+\infty): \delta = \frac{2(1+K\alpha)}{d+K(\alpha d-b)}, \delta \neq \frac{2}{r}\right\}.$$

At $E_2(x^*,y^*)$, we write equation (7) as

$$F(\lambda) := \lambda^2 - (2+\Delta\delta)\lambda + (1+\Delta\delta+\Omega\delta^2) = 0,$$

where

$$\Delta = r - \frac{2rx^*}{K} + \frac{ay^*}{(1+\alpha x^*)^2(1+\beta y^*)} + \frac{bx^* - d(1+\alpha x^*)(1+\beta y^*)^2}{(1+\alpha x^*)(1+\beta y^*)^2},$$

$$\Omega = \frac{1}{(1+\alpha x^*)^2(1+\beta y^*)^3}\left(abx^*y^* - ay^*\right.$$
$$+ \frac{1}{K(1+\alpha x^*)^2(1+\beta y^*)^3}\left(r(K-2\right.$$

Then $F(1) = \Omega\delta^2 > 0$ and $F(-1) = 4 + 2\Delta\delta + \Omega\delta^2$.
We state following Proposition about stability criterion of E_2.

Proposition 2.3 *Suppose that fixed point* $E_2(x^*,y^*)$ *of system (2) exists. Then it is a*

(i) sink if one of the following conditions holds

(i.1) $\Delta^2 - 4\Omega \geq 0$ and $\delta < \frac{-\Delta-\sqrt{\Delta^2-4\Omega}}{\Omega}$;

(i.2) $\Delta^2 - 4\Omega < 0$ *and* $\delta < -\frac{\Delta}{\Omega}$;

(ii) source if one of the following conditions holds

(ii.1) $\Delta^2 - 4\Omega \geq 0$ and $\delta > \frac{-\Delta+\sqrt{\Delta^2-4\Omega}}{\Omega}$;

(ii.2) $\Delta^2 - 4\Omega < 0$ *and* $\delta > -\frac{\Delta}{\Omega}$;

(iii) non-hyperbolic if one of the following conditions holds

(iii.1) $\Delta^2 - 4\Omega \geq 0$ and $\delta = \frac{-\Delta\pm\sqrt{\Delta^2-4\Omega}}{\Omega}$;

(iii.2) $\Delta^2 - 4\Omega < 0$ *and* $\delta = -\frac{\Delta}{\Omega}$;

(iv) saddle if otherwise.

From Proposition 2.3, we see that two eigenvalues of $J(E_2)$ are $\lambda_1 = -1$ and $\lambda_2 \neq -1,1$ if condition (iii.1) holds. We rewrite the term (iii.1) as follows

$$FB^1_{E_2} = \left\{(r,K,a,b,d,\alpha\beta,\delta) \in (0,+\infty): \delta = \frac{-\Delta - \sqrt{\Delta^2 - 4\Omega}}{\Omega}, \quad \Delta^2 - 4\Omega \geq 0\right\},$$

or

$$FB^2_{E_2} = \left\{(r,K,a,b,d,\alpha\beta,\delta) \in (0,+\infty): \delta = \frac{-\Delta + \sqrt{\Delta^2 - 4\Omega}}{\Omega}, \quad \Delta^2 - 4\Omega \geq 0\right\}.$$

Therefore, a flip bifurcation can appear at E_2 if parameters vary arround the set $FB^1_{E_2}$ or $FB^2_{E_2}$.

Also we rewrite the term (iii.2) as follows

$$NSB_{E_2} = \left\{(r,K,a,b,d,\alpha\beta,\delta) \in (0,+\infty): \delta = -\frac{\Delta}{\Omega}, \quad \Delta^2 - 4\Omega < 0\right\},$$

and if the parameters change in small vicinity of NSB_{E_2}, two eigenvalues $\lambda_{1,2}$ of $J(E_2)$ are complex having magnitude one and then NS bifurcation can emerge from fixed point E_2.

3 Bifurcation Analysis

In this section, we will give attention to recapitulate bifurcations (flip and Neimark-Sacker) of system (2) around E_2 by using the theory of bifurcation (Kuzenetsov, 1998; Winggins, 2003). We set δ as a bifurcation parameter.

3.1 Flip bifurcation

Consider the system (2) at the fixed point $E_2(x^*, y^*)$ with arbitrary parameter $(r,K,a,b,d,\alpha\beta,\delta) \in FB^1_{E_2}$. Similar fashion for the case of $FB^2_{E_2}$. Since the parameters lie in $FB^1_{E_2}$, let $\delta = \delta_F = \frac{-\Delta-\sqrt{\Delta^2-4\Omega}}{\Omega}$, then the eigenvalues of positive fixed point (x^*, y^*) are

$$\lambda_1(\delta_F) = -1 \quad \text{and} \quad \lambda_2(\delta_F) = 3 + \Delta\delta_F.$$

The condition $|\lambda_2(\delta_F)| \neq 1$ leads to

$$\Delta\delta_F \neq -2, -4 \tag{9}$$

Using the transformation $\tilde{x} = x - x^*$, $\tilde{y} = y - y^*$ and writing $A(\delta) = J(x^*, y^*)$, we shift the fixed point (x^*, y^*) of system (2) to the origin. After Taylor expansion, system (2) reduces to

$$\begin{pmatrix}\tilde{x}\\ \tilde{y}\end{pmatrix} \to A(\delta)\begin{pmatrix}\tilde{x}\\ \tilde{y}\end{pmatrix} + \begin{pmatrix}F_1(\tilde{x},\tilde{y},\delta)\\ F_2(\tilde{x},\tilde{y},\delta)\end{pmatrix} \tag{10}$$

where $X = (\tilde{x}, \tilde{y})^T$ and

$$
\begin{aligned}
F_1(\tilde{x},\tilde{y},\delta) &= \frac{1}{6}\Big[-\frac{6\delta a\beta^2x^*}{(1+\alpha x^*)(1+\beta y^*)^4}\tilde{y}^3+\frac{2\delta a\beta}{(1+\alpha x^*)^2(1+\beta y^*)^3}\tilde{x}\tilde{y}^2+\frac{2\delta a\alpha}{(1+\alpha x^*)^3(1+\beta y^*)^2}\tilde{x}^2\tilde{y}-\frac{6\delta a\alpha^2y^*}{(1+\alpha x^*)^4(1+\beta y^*)}\tilde{x}^3\Big]\\
&\quad+\frac{1}{2}\Big[\frac{2\delta a\beta x^*}{(1+\alpha x^*)(1+\beta y^*)^3}\tilde{y}^2-\frac{2\delta a}{(1+\alpha x^*)^2(1+\beta y^*)^2}\tilde{x}\tilde{y}+\Big(-\frac{2r}{K}+\frac{2\delta a\alpha y^*}{(1+\alpha x^*)^3(1+\beta y^*)}\Big)\tilde{x}^2\Big]+O(\|X\|^4)\\
F_2(\tilde{x},\tilde{y},\delta) &= \frac{1}{6}\Big[\frac{6\delta b\beta^2x^*}{(1+\alpha x^*)(1+\beta y^*)^4}\tilde{y}^3-\frac{2\delta b\beta}{(1+\alpha x^*)^2(1+\beta y^*)^3}\tilde{x}\tilde{y}^2-\frac{2\delta b\alpha}{(1+\alpha x^*)^3(1+\beta y^*)^2}\tilde{x}^2\tilde{y}+\frac{6\delta b\alpha^2y^*}{(1+\alpha x^*)^4(1+\beta y^*)}\tilde{x}^3\Big]\\
&\quad+\frac{1}{2}\Big[-\frac{2\delta b\beta x^*}{(1+\alpha x^*)(1+\beta y^*)^3}\tilde{y}^2+\frac{2\delta b}{(1+\alpha x^*)^2(1+\beta y^*)^2}\tilde{x}\tilde{y}-\frac{2\delta b\alpha x^*}{(1+\alpha x^*)^3(1+\beta y^*)}\tilde{x}^2\Big]+O(\|X\|^4)
\end{aligned}
\tag{11}
$$

It follows that

$$
\begin{aligned}
B_1(x,y) &= \sum_{j,k=1}^{2}\frac{\delta^2F_1(\xi,\delta)}{\delta\xi_j\delta\xi_k}\Big|_{\xi=0}x_jy_k\\
&= \frac{2\delta a\beta x^*}{(1+\alpha x^*)(1+\beta y^*)^3}x_2y_2-\frac{\delta a}{(1+\alpha x^*)^2(1+\beta y^*)^2}(x_1y_2+x_2y_1)+\Big(-\frac{2r}{K}+\frac{2\delta a\alpha y^*}{(1+\alpha x^*)^3(1+\beta y^*)}\Big)x_1y_1,\\
B_2(x,y) &= \sum_{j,k=1}^{2}\frac{\delta^2F_2(\xi,\delta)}{\delta\xi_j\delta\xi_k}\Big|_{\xi=0}x_jy_k\\
&= -\frac{2\delta b\beta x^*}{(1+\alpha x^*)(1+\beta y^*)^3}x_2y_2+\frac{\delta b}{(1+\alpha x^*)^2(1+\beta y^*)^2}(x_1y_2+x_2y_1)-\frac{2\delta a\alpha y^*}{(1+\alpha x^*)^3(1+\beta y^*)}x_1y_1,
\end{aligned}
$$

$$
\begin{aligned}
C_1(x,y,u) &= \sum_{j,k,l=1}^{2}\frac{\delta^2F_1(\xi,\delta)}{\delta\xi_j\delta\xi_k\delta\xi_l}\Big|_{\xi=0}x_jy_ku_l\\
&= -\frac{6\delta a\beta^2x^*}{(1+\alpha x^*)(1+\beta y^*)^4}x_2y_2u_2-\frac{6\delta a\alpha^2y^*}{(1+\alpha x^*)^4(1+\beta y^*)}x_1y_1u_1\\
&\quad+\frac{2\delta a\alpha}{(1+\alpha x^*)^3(1+\beta y^*)^2}(x_1y_2u_1+x_2y_1u_1+x_1y_1u_2)+\frac{2\delta a\beta}{(1+\alpha x^*)^2(1+\beta y^*)^3}(x_1y_2u_2\\
&\quad+x_2y_1u_2+x_2y_2u_1)\\
C_2(x,y,u) &= \sum_{j,k,l=1}^{2}\frac{\delta^2F_2(\xi,\delta)}{\delta\xi_j\delta\xi_k\delta\xi_l}\Big|_{\xi=0}x_jy_ku_l\\
&= \frac{6\delta b\beta^2x^*}{(1+\alpha x^*)(1+\beta y^*)^4}x_2y_2u_2+\frac{6\delta b\alpha^2y^*}{(1+\alpha x^*)^4(1+\beta y^*)}x_1y_1u_1\\
&\quad-\frac{2\delta b\alpha}{(1+\alpha x^*)^3(1+\beta y^*)^2}(x_1y_2u_1+x_2y_1u_1+x_1y_1u_2)-\frac{2\delta b\beta}{(1+\alpha x^*)^2(1+\beta y^*)^3}(x_1y_2u_2\\
&\quad+x_2y_1u_2+x_2y_2u_1)
\end{aligned}
$$

and $\delta=\delta_F$.

Therefore, we obtain the following symmetric multilinear vector functions of $x,y,u\in\mathbb{R}^2$:

$B(x,y)=\begin{pmatrix}B_1(x,y)\\B_2(x,y)\end{pmatrix}$and $(x,y,u)=\begin{pmatrix}C_1(x,y,u)\\C_2(x,y,u)\end{pmatrix}$.

Let $p,q\in\mathbb{R}^2$ be two eigenvectors of A for eigenvalue $\lambda_1(\delta_F)=-1$ such that $A(\delta_F)q=-q$ and $A^T(\delta_F)p=-p$. Then by direct calculation we get

$$
q\sim\Big(2-d\delta_F+\frac{b\delta_Fx^*}{(1+\alpha x^*)(1+\beta y^*)^2},-\frac{b\delta_Fy^*}{(1+\alpha x^*)^2(1+\beta y^*)}\Big)^T,
$$

$$p\sim\left(2-d\delta_F+\frac{b\delta_F x^*}{(1+\alpha x^*)(1+\beta y^*)^2},\frac{a\delta_F x^*}{(1+\alpha x^*)(1+\beta y^*)^2}\right)^T.$$

We set $p=\gamma_1\left(2-d\delta_F+\frac{b\delta_F x^*}{(1+\alpha x^*)(1+\beta y^*)^2},\frac{a\delta_F x^*}{(1+\alpha x^*)(1+\beta y^*)^2}\right)^T$, where

$$\gamma_1=\frac{1}{\left(2-d\delta_F+\frac{b\delta_F x^*}{(1+\alpha x^*)(1+\beta y^*)^2}\right)^2-\frac{ab\delta_F^2 x^* y^*}{(1+\alpha x^*)^3(1+\beta y^*)^3}}.$$

Then by the standard scalar product in $\mathbb{R}^2$ defined by $\langle p,q\rangle=p_1q_1+p_2q_2$, we show that $\langle p,q\rangle=1$. The direction of the flip bifurcation is obtained by the sign $c(\delta_F)$, the coefficient of critical normal form (Kuzenetsov, 1998) and is given by

$$c(\delta_F)=\frac{1}{6}\langle p,C(q,q,q)\rangle-\frac{1}{2}\langle p,B(q,(A-I)^{-1}B(q,q))\rangle \quad (12)$$

We state the following result on flip bifurcation according to above analysis.

Theorem 3.1 *If (9) holds, $c(\delta_F)\neq 0$ and the parameter δ changes its value around δ_F, then system (2) undergoes a flip bifurcation at positive fixed point $E_2(x^*,y^*)$. Moreover, the period-2 orbits that bifurcate from $E_2(x^*,y^*)$ are stable (resp., unstable) if $c(\delta_F)>0$ (resp., $c(\delta_F)<0$).*

3.2 Neimark-Sacker bifurcation

Next, we consider system (2) at fixed point $E_2(x^*,y^*)$ with arbitrary $(r,K,a,b,d,\alpha\beta,\delta)\in NSB_{E_2}$. From equation (7), the eigenvalues are given by

$$\lambda,\bar{\lambda}=\frac{-p(\delta)\pm\sqrt{p(\delta)^2-4q(\delta)}}{2}.$$

Since the parameters belong to NSB_{E_2}, so the eigenvalues will be complex and

$$\lambda,\bar{\lambda}=1+\frac{\Delta\delta}{2}\pm\frac{i\delta}{2}\sqrt{4\Omega-\Delta^2},$$

Let

$$\delta=\delta_{NS}=-\frac{\Delta}{\Omega} \quad (13)$$

Therefore, we have

$$|\lambda|=\sqrt{q(\delta)},\quad q(\delta_{NS})=1,\quad \left.\frac{d|\lambda(\delta)|}{d\delta}\right|_{\delta=\delta_{NS}}=-\frac{\Delta}{2}\neq 0 \quad (14)$$

Moreover, if $p(\delta_{NS})\neq 0,1$, then

$$\frac{\Delta^2}{\Omega}\neq 2,3 \quad (15)$$

which obviously satisfies

$$\lambda^k(\delta_{NS}) \neq 1 \quad \text{for } k = 1,2,3,4 \tag{16}$$

Suppose $q, p \in \mathbb{C}^2$ are two eigenvectors of $A(\delta_{NS})$ and $A^T(\delta_{NS})$ for eigenvalues $\lambda(\delta_{NS})$ and $\bar{\lambda}(\delta_{NS})$ such that

$$A(\delta_{NS})q = \lambda(\delta_{NS})q, \quad A(\delta_{NS})\bar{q} = \bar{\lambda}(\delta_{NS})\bar{q}$$

and

$$A^T(\delta_{NS})p = \bar{\lambda}(\delta_{NS})p, \quad A^T(\delta_{NS})\bar{p} = \lambda(\delta_{NS})\bar{p}.$$

Then by direct computation we obtain

$$q \sim \left(1 - \lambda - d\delta_{NS} + \frac{b\delta_{NS}x^*}{(1+\alpha x^*)(1+\beta y^*)^2}, -\frac{b\delta_{NS}y^*}{(1+\alpha x^*)^2(1+\beta y^*)}\right)^T,$$

$$p \sim \left(1 - \bar{\lambda} - d\delta_{NS} + \frac{b\delta_{NS}x^*}{(1+\alpha x^*)(1+\beta y^*)^2}, \frac{a\delta_{NS}x^*}{(1+\alpha x^*)(1+\beta y^*)^2}\right)^T.$$

We set $p = \gamma_2\left(1 - \bar{\lambda} - d\delta_{NS} + \frac{b\delta_{NS}x^*}{(1+\alpha x^*)(1+\beta y^*)^2}, \frac{a\delta_{NS}x^*}{(1+\alpha x^*)(1+\beta y^*)^2}\right)^T$, where

$$\gamma_2 = \frac{1}{\left(1 - \bar{\lambda} - d\delta_{NS} + \frac{b\delta_{NS}x^*}{(1+\alpha x^*)(1+\beta y^*)^2}\right)^2 - \frac{ab\delta_{NS}^2 x^* y^*}{(1+\alpha x^*)^3(1+\beta y^*)^3}}.$$

Then it is clear that $\langle p, q\rangle = 1$ where $\langle p, q\rangle = \bar{p}_1 q_2 + \bar{p}_2 q_1$ for $p, q \in \mathbb{C}^2$. Now, we decompose vector $X \in \mathbb{R}^2$ as $X = zq + \bar{z}\bar{q}$, for δ close to δ_{NS} and $z \in \mathbb{C}$. Obviously, $z = \langle p, X\rangle$. Thus, we obtain the following transformed form of system (10) for $|\delta|$ near δ_{NS}:

$$z \mapsto \lambda(\delta)z + g(z, \bar{z}, \delta),$$

where $\lambda(\delta) = (1 + \varphi(\delta))e^{i\theta(\delta)}$ with $\varphi(\delta_{NS}) = 0$ and $g(z, \bar{z}, \delta)$ is a smooth complex-valued function. After Taylor expression of g with respect to $(z, \bar{z})$, we obtain

$$g(z, \bar{z}, \delta) = \sum_{k+l\geq 2} \frac{1}{k!\, l!} g_{kl}(\delta) z^k \bar{z}^l, \quad \text{with} \quad g_{kl} \in \mathbb{C}, \qquad k, l = 0,1,\cdots.$$

According to multilinear symmetric vector functions, the coefficients g_{kl} are

$$g_{20}(\delta_{NS}) = \langle p, B(q, q)\rangle, \quad g_{11}(\delta_{NS}) = \langle p, B(q, \bar{q})\rangle$$
$$g_{02}(\delta_{NS}) = \langle p, B(\bar{q}, \bar{q})\rangle, \quad g_{21}(\delta_{NS}) = \langle p, C(q, q, \bar{q})\rangle,$$

The invariant closed curve appear in the direction which is determined by the coefficient $a(\delta_{NS})$ and calculated via

$$a(\delta_{NS}) = \mathrm{Re}\left(\frac{e^{-i\theta(\delta_{NS})}g_{21}}{2}\right) - \mathrm{Re}\left(\frac{(1 - 2e^{i\theta(\delta_{NS})})e^{-2i\theta(\delta_{NS})}}{2(1 - e^{i\theta(\delta_{NS})})} g_{20}g_{11}\right) - \frac{1}{2}|g_{11}|^2 - \frac{1}{4}|g_{02}|^2,$$

where $e^{i\theta(\delta_{NS})} = \lambda(\delta_{NS})$.

It is clear that the conditions (14) and (16) known as transversal and nondegenerate for system (2) hold well. We obtain the following result.

Theorem 3.2 *If (15) holds,* $a(\delta_{NS}) \neq 0$ *and the parameter* δ *changes its value in small vicinity of* NSB_{E_2}*, then system (2) passes through a Neimark-Sacker bifurcation at positive fixed point* E_2*. Moreover, if* $a(\delta_{NS}) < 0$ *(resp.,* > 0*), then there exists a unique attracting (resp., repelling) invariant closed curve bifurcates from* E_2*.*

4 Numerical Simulations

Here, bifurcation diagrams, phase portraits, maximum Lyapunov exponents and fractal dimension of system (2) will be drawn to validate our theoretical results using numerical simulation. We assume that δ is a bifurcation parameter unless stated. We consider parameter values in the following examples for bifurcation analysis:

Example 1 We fix the parameters $r = 1.75, K = 1.0, a = 1.0, b = 1.1, d = 0.2, \alpha = 0.98, \beta = 0.5$ and varying δ in range $2.4 \leq \delta \leq 3.15$. By calculation, we find that the fixed point ystem (2) is $E_2(0.623837, 2.25864)$, and the critical point for flip bifurcationa is $\delta = \delta_F \sim 2.54621$. At the critical bifurcation point, the two eigenvalues are $\lambda_1 = -1, \lambda_2 = 0.586109$, $a(\delta_F) = 28.7908$ and $(r, K, a, b, d, \alpha\beta, \delta) \in FB^1_{E_2}$. This verifies Theorem 3.1.

According to bifurcation diagrams shown in Fig. 1(a-b), we see that stability of fixed point E_2 happens for $\delta < 2.54621$, loses its stability at $\delta = 2.54621$ and a period doubling phenomena lead to chaos for $\delta > 2.54621$. The maximum Lyapunov exponents and fractal dimension related to Fig. 1(a-b) are computed and shown in Fig. 1(c-d). We observe that the period -2,- 4, -8 orbits occur for $\delta \in [2.4, 3.026]$, chaotic set for $\delta \in [3.026, 3.15]$. As determined by the maximum Lyapunov exponent, the status of stable, periodic or chaotic dynamics are compatible with sign in Fig. 1(c-d).

Example 2 We fix the parameters $r = 1.5, K = 1.9, a = 1.5, b = 1.95, d = 2.0, \alpha = 0.1, \beta = 0.1$; and varying δ in range $0.75 \leq \delta \leq 1.4$. After calculation, we observe that a Neimark-Sacker (NS) bifurcation appears at fixed point $(1.19809, 0.43154)$ for $\delta = \delta_{NS} \sim 0.948329$. Also, we have $\lambda, \bar{\lambda} = 0.573827 \pm 0.818977i$, $g_{20} = 0.127352 - 0.636909i$, $g_{11} = 0.699069 - 0.685987i$, $g_{02} = 1.01789 + 1.75825i$, $g_{21} = -0.0398675 + 0.0242444i$, $a(\delta_{NS}) = -1.50356$ and $(r, K, a, b, d, \alpha\beta, \delta) \in NSB_{E_2}$. This verifies Theorem 3.2.

The bifurcation diagrams shown in Fig. 2(a-b) demonstrate that stability of E_2 happens for $\delta < 0.948329$, loses its stability at $\delta = 0.948329$ and an attracting invariant curve appears if $\delta > 0.948329$. We dispose the maximum Lyapunov exponents in Fig. 2(c) relating bifurcation in Fig. 2(a-b), which confirm the existences of chaos and period window as parameter δ varying. When $\delta \sim 1.4$, the sign of maximum Lyapunov exponent confirming presence of chaos. Fig. 2(d) is local amplification of Fig. 2(a) for $\delta \in [1.27, 1.35]$.

The phase portraits of bifurcation diagrams in Fig. 2(a-b) for different values of δ are displayed in Fig. 3, which clearly illustrates the act of smooth invariant curve how it bifurcates from the stable fixed point and increases its radius. As δ grows, disappearance of closed curve occurs suddenly and a period- 6, 11, 17, and period 51 orbits appear at $\delta \sim 1.075$, $\delta \sim 1.3545$, $\delta \sim 1.2765$ and $\delta \sim 1.3155$ respectively. We also see that a fully developed chaos in system (2) occurs at $\delta \sim 1.4$.

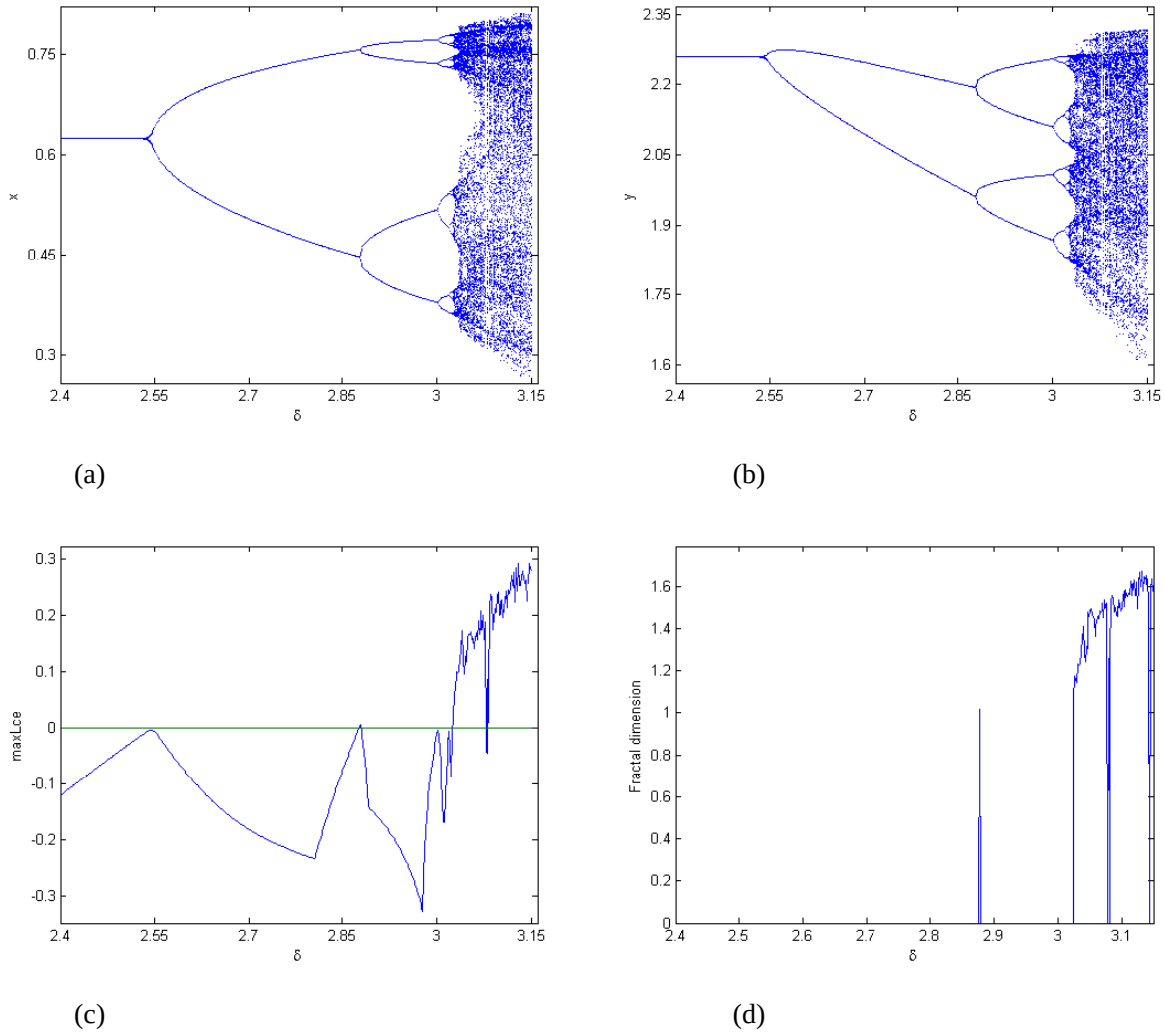

(a) (b)

(c) (d)

Fig. 1 Flip bifurcation and Lyapunov exponent of system (2). (a) bifurcation for prey, (b) bifurcation for predator, (c) maximum Lyapunov exponents related to (a-b), (d) Fractal dimension corresponding to (a). Initial value $(x_0, y_0) = (0.604, 2.24)$.

With the variation of other parameter values (e.g., parameter r), the predator-prey system may exhibit richer dynamical behaviors in the Neimark-Sacker bifurcation diagram. When we set the parameter values as given in case (ii) with $r = 1.65$, a new Neimark-Sacker bifurcation diagram is obtained as disposed in Fig. 4(a-b). The system undergoes Neimark-Sacker bifurcation at $\delta = 0.956099$. Similar nonlinear characteristics to Figures 2 and 3 are found in this case, such as route to chaos, invariant curves, chaotic attractors, and periodic windows. The maximum Lyapunov exponent corresponding to Fig. 4(a-b) is computed and plotted in Fig. 4(c), which confirm the existences of chaos and period window as parameter δ varying. The local amplification diagram corresponding to Fig. 4(a) for $\delta \in [1.21, 1.37]$ is shown in Fig. 2(c). We observe from Fig. 4(a-b) that stability of syatem (2) happens for $\delta < 0.956099$, loses its stability at $\delta = 0.956099$ and an attracting invariant curve appears if $\delta > 0.956099$. The phase portraits of bifurcation diagrams in Fig. 4(a-b) for different values of δ are displayed in Fig. 5. Also, we observe in this case that there are period- 5, 6, 15, 16, and period 21 orbits and attracting chaotic sets.

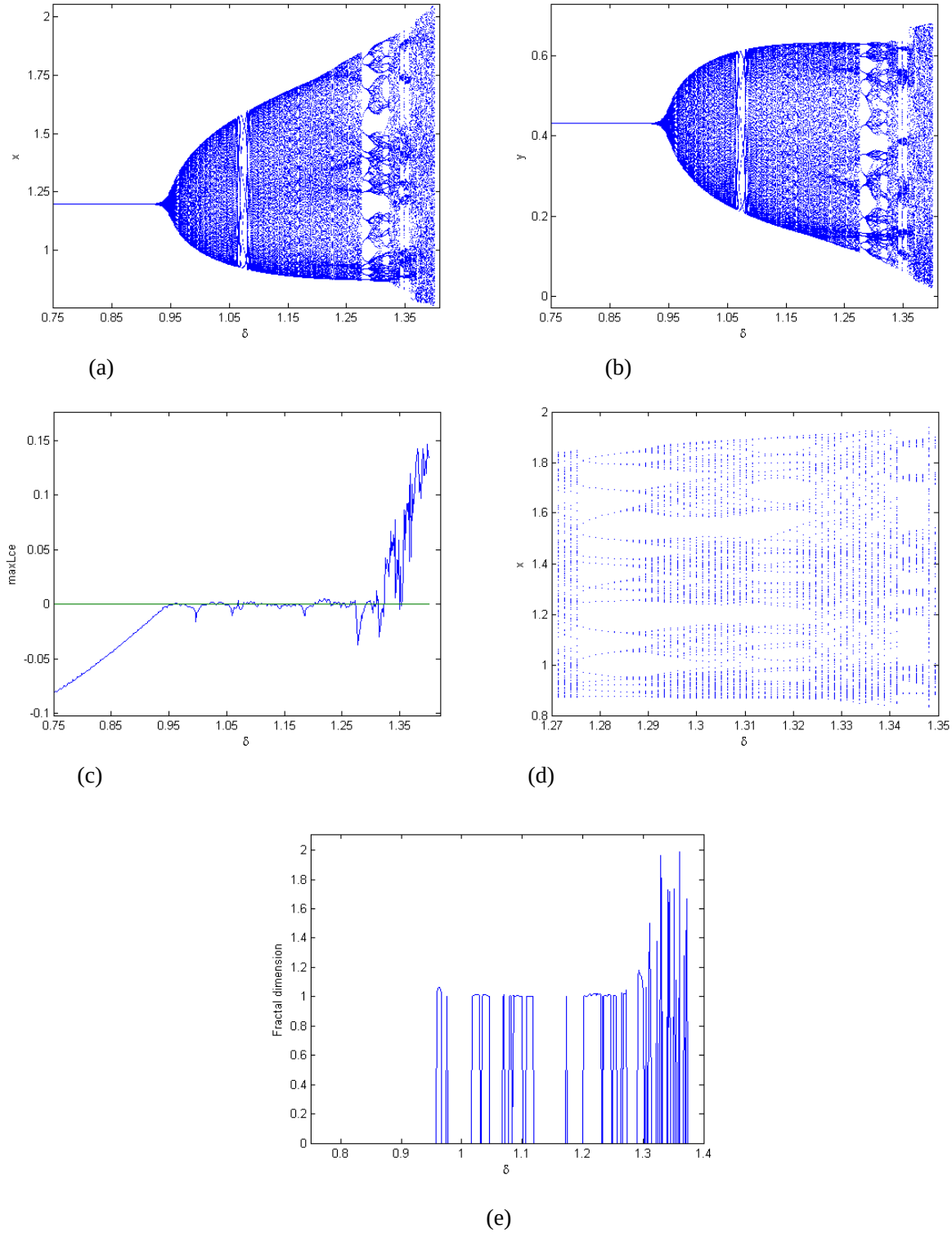

Fig. 2 NS bifurcation and Lyapunov exponent of system (2). (a) NS bifurcation for prey, (b) NS bifurcation for predator, (c) maximum Lyapunov exponents related to (a-b), (d) local amplification diagram in (a) for $\delta \in [1.27,1.35]$, (e) Fractal dimension associated with (a). Initial value $(x_0, y_0) = (1.17,035)$.

Fig. 6 shows the Neimark-Sacker bifurcation diagram when the parameter values are given as in case (ii) with $r = 1.85$. The critical Neimark-Sacker bifurcation point is $\delta = 0.966328$, and the first chaotic point is

at around $\delta = 1.322$ (Fig. 7). On the route to chaos, periodic windows with period- 5, 7, 10, and period 28 orbits and narrow chaotic band are found. On each branch, the predator-prey system sequentially undergoes sub-Neimark-Sacker bifurcation, flip bifurcation and periodic window with the increase of δ value.

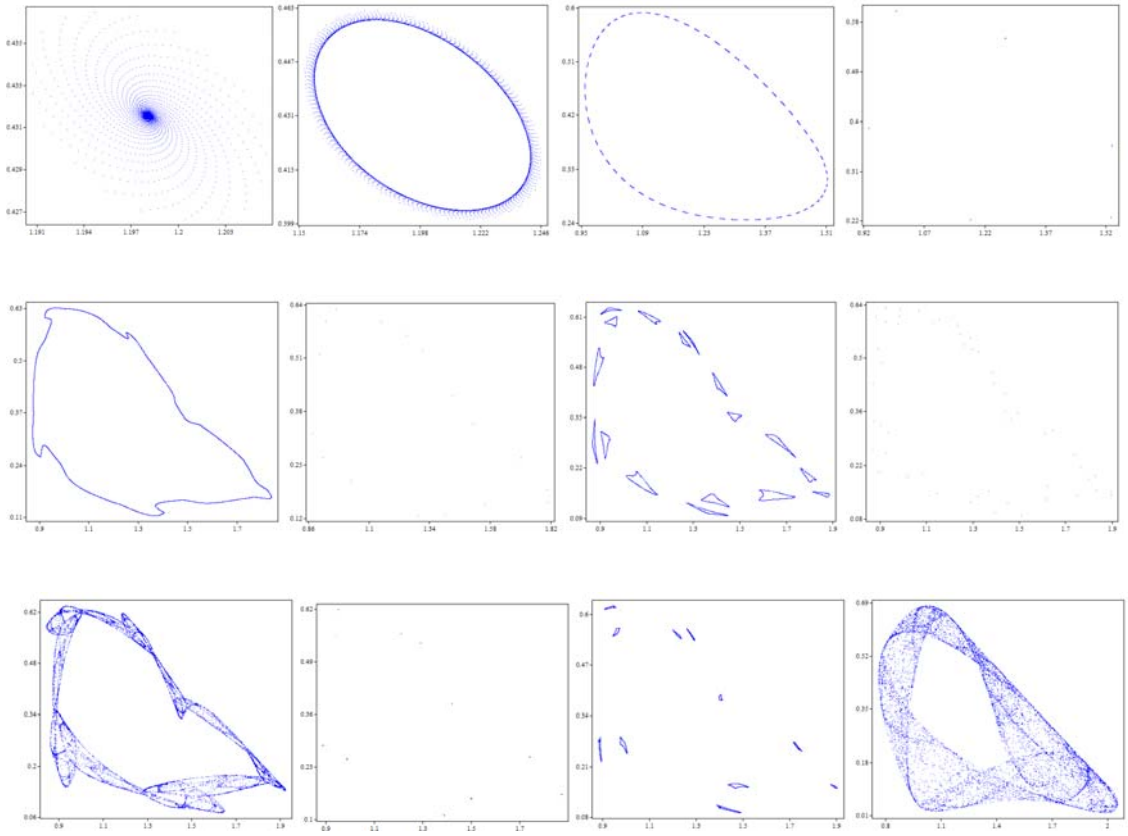

Fig. 3 Phase portraits (xy-plane) of bifurcation diagrams Fig. 2(a-b) for different values of δ.

Example 3 We fix the parameters $K = 1.9, a = 1.5, b = 1.95, d = 2.0, \alpha = 0.1, \beta = 0.1$; and varying δ in range $0.75 \leq \delta \leq 1.4$, and r in range $1.5 \leq r \leq 1.85$. The dynamic complexity of system (2) can be observed when more parameters vary. The three-dimensional bifurcation diagrams of system (2) for control parameters $\delta \in [0.75,1.4]$, $r \in [1.5,1.85]$ and fixing remaining parameters as in case (ii), are shown in Fig. 8 (a). The 2D projection of 3D maximum Lyapunov exponents for two control parameters onto (δ, r) plane is plotted in Fig. 8(b). It is easy to find values of control parameters for which the dynamics of system (2) is in status of non-chaotic, periodic or chaotic. For instance, there is a chaotic dynamics for $\delta = 1.4$, $r = 1.5$, and the non-chaotic dynamics for $\delta = 0.9$, $r = 1.5$ (see Fig. 3), which are compatible with the signs of maximum Lyapunov exponents in Fig. 8 (b). As shown in Fig. 8 (a), we find that, with the increase of parameter r, the Neimark-Sacker bifurcation diagram moves toward the positive δ axis. Such movement takes the increase of Neimark-Sacker bifurcation critical point and first chaotic point and simultaneously changes the periodic windows on the route to chaos.

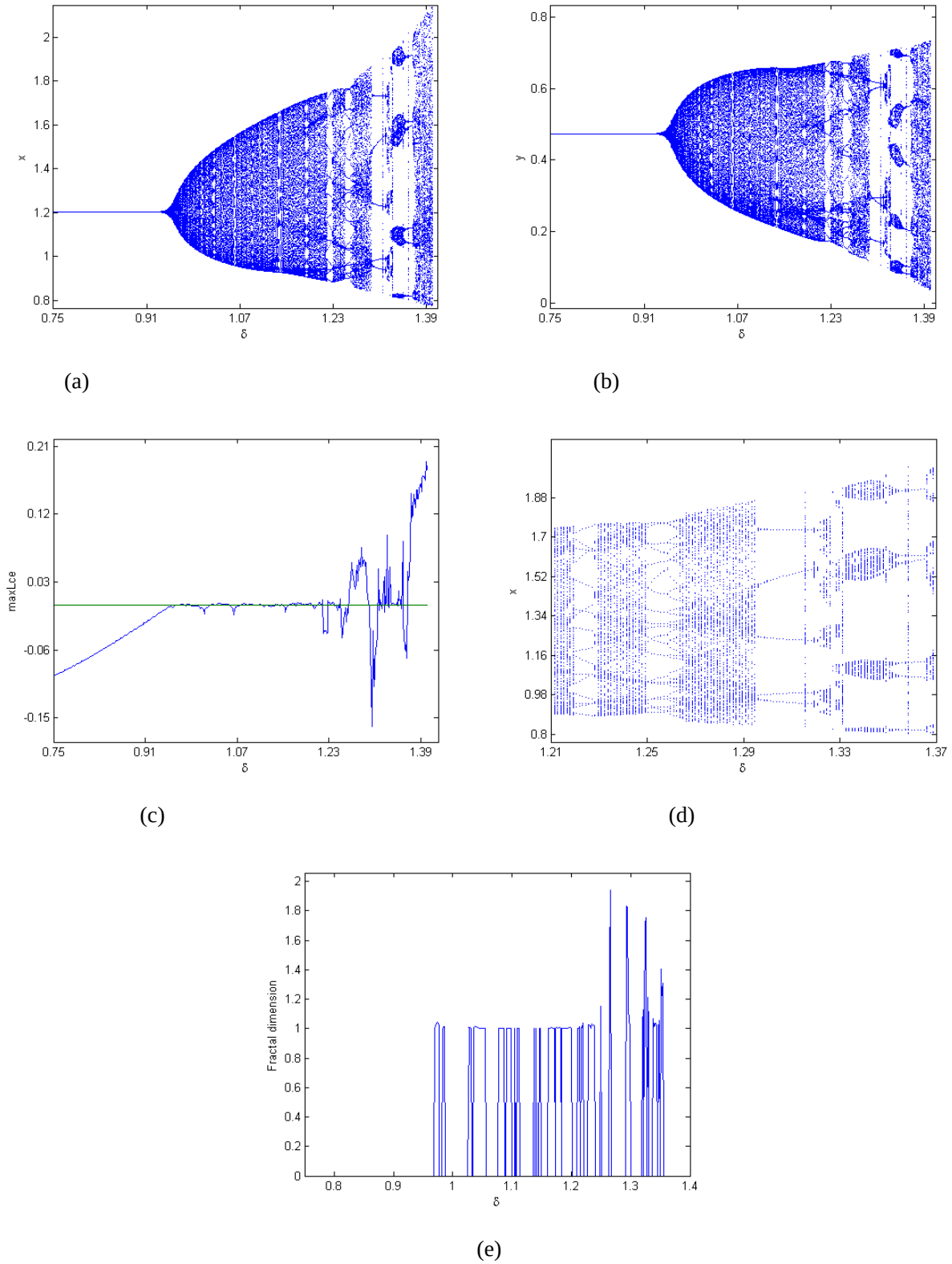

Fig. 4 NS bifurcation and Lyapunov exponent of system (2). (a) NS bifurcation for prey, (b) NS bifurcation for predator, (c) maximum Lyapunov exponents related to (a-b), (d) local amplification diagram in (a) for $\delta \in [1.21,1.37]$ (e) Fractal dimension associated with (a). Initial value $(x_0, y_0) = (1.17,035)$.

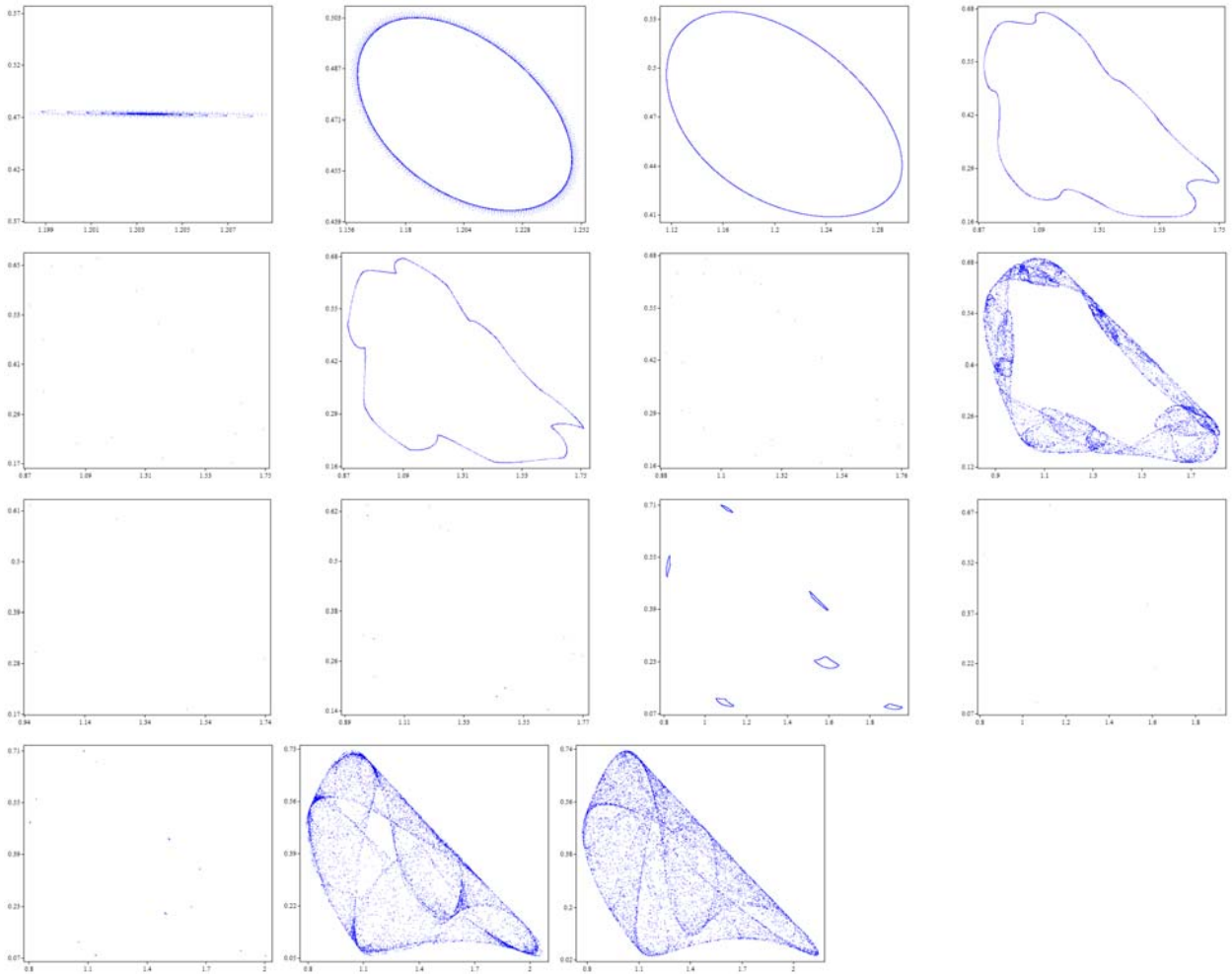

Fig. 5 Phase portraits (xy-plane)of bifurcation diagrams Fig. 4(a-b) for different values of δ.

Example 4 We fix the parameters $r = 1.5, K = 1.9, a = 1.5, b = 1.95, d = 2.0, \delta = 1.3$; and varying α in range $0.04 \leq \alpha \leq 0.2$, and β in range $0.1 \leq \beta \leq 0.5$. The three-dimensional bifurcation diagrams of system (2) for control parameters $\alpha \in [0.04,0.2]$, $\beta \in [0.1,0.5]$ and fixing fixing $r = 1.5, K = 1.9, a = 1.5, b = 1.95, d = 2.0, \delta = 1.3$, are shown in Fig. 8 (c). The 2D projection of 3D maximum Lyapunov exponents for two control parameters onto (δ, r) plane is plotted in Fig. 8(d). We observe that the increases values of control parameters α and β, the dynamics of system (2) changes from chaotic to non-chaotic status. Moreover, we find that the predator-prey system experiences flip bifurcation and Neimark- Sacker bifurcation combine together.

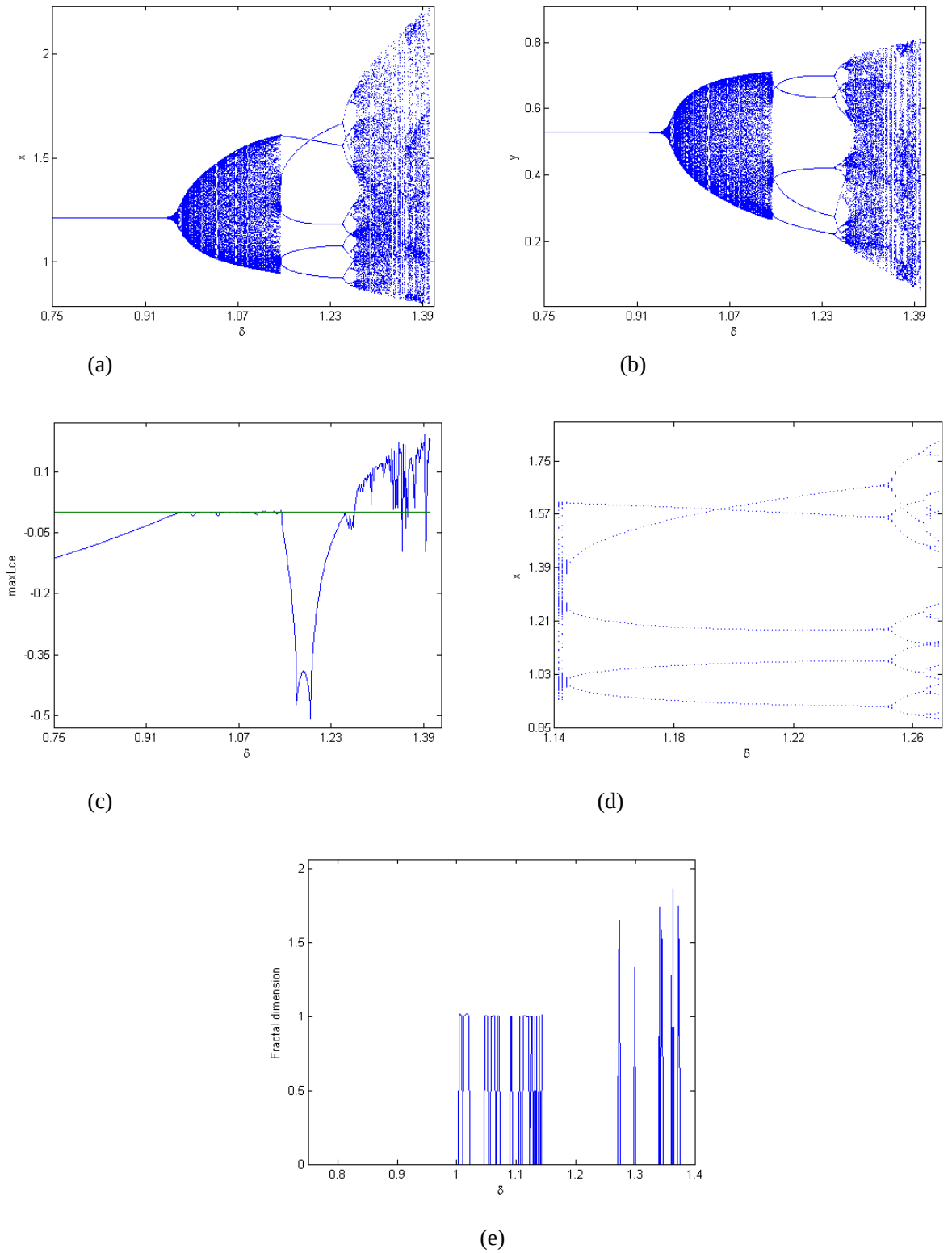

Fig. 6 NS bifurcation and Lyapunov exponent of system (2). (a) NS bifurcation for prey, (b) NS bifurcation for predator, (c) maximum Lyapunov exponents related to (a-b), (d) local amplification diagram in (a) for $\delta \in [1.14,1.27]$ (e) Fractal dimension associated with (a). Initial value $(x_0, y_0) = (1.17,035)$.

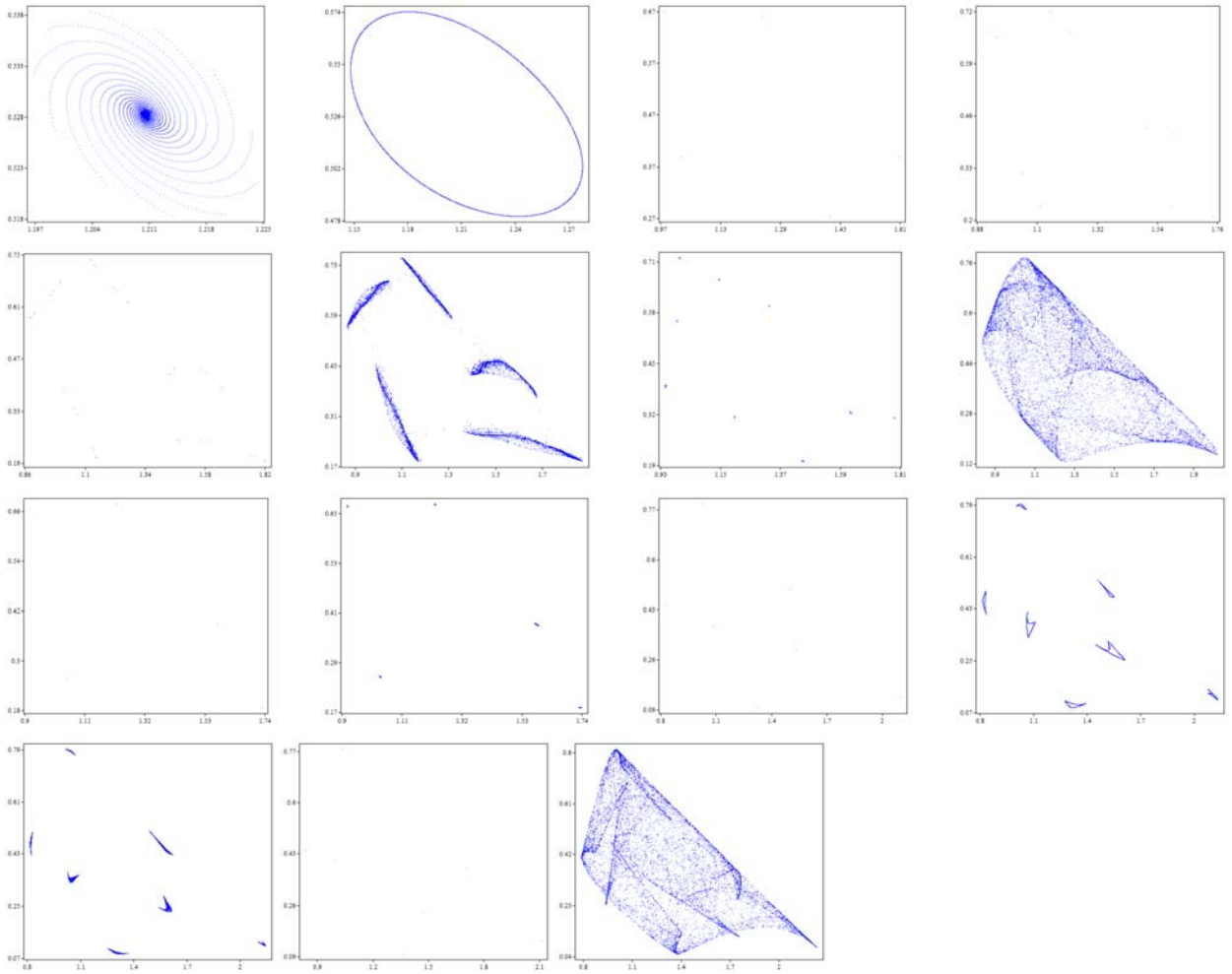

Fig. 7 Phase portraits(xy-plane)of bifurcation diagrams Fig. 6(a-b) for different values of δ.

The measure of fractal dimensions characterizes the strange attractors of a system. By using Lyapunov exponents, the fractal dimension (Cartwright, 1999; Kaplan and Yorke, 1979) is defined by

$$d_L = j + \frac{\sum_{i=1}^{j} h_i}{|h_j|}$$

where $h_1, h_2, \ldots, h_n$ are Lyapunov exponents and j is the largest integer such that $\sum_{i=1}^{j} h_i \geq 0$ and $\sum_{i=1}^{j+1} h_i < 0$.

For our two-dimensional system (2), the fractal dimension takes the form

$$d_L = 1 + \frac{h_1}{|h_2|}, \quad h_1 > 0 > h_2.$$

With parameter values as in case (ii), the fractal dimension of system (2) is plotted in Fig. 2(e). The strange attractors given in Fig. 3 and its corresponding fractal dimension illustrate that the Leslie type predator-prey system (2) has a chaotic dynamics as the parameter δ increases.

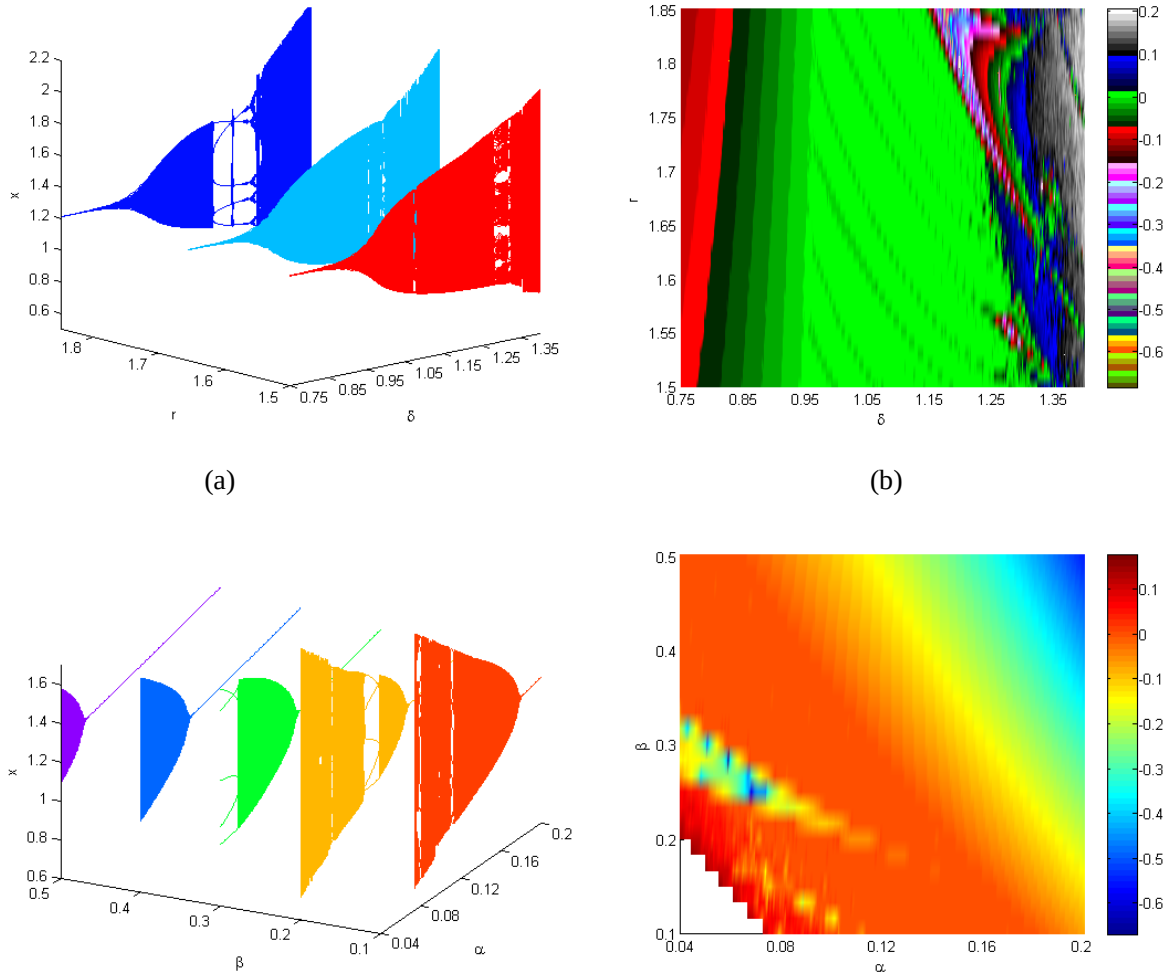

Fig. 8 Diagnostic of system (2) for control parameters δ and r. (a) bifurcation for prey covering $\delta \in [0.75,1.4]$, $r = 1.5,1.65$ and 1.85 in $(\delta - r - x)$ space (b) The 2D projection of 3D maximum Lyapunov exponents onto (δ, r) plane. (c) bifurcation for prey covering $\alpha \in [0.04,0.2]$, $\beta = 0.1,0.2,0.3,0.4$ and 0.5 in $(\alpha - \beta - x)$ space (d) The 2D projection of 3D maximum Lyapunov exponents onto (δ, r) plane. Initial value $(x_0, y_0) = (1.17,035)$.

5 Chaos Control

To stabilize chaos at the state of unstable trajectories of system (2), a state feedback control method (Elaydi, 1996) is applied. By adding a feedback control law as the control force u_n to system (2), the controlled form of system (2) becomes

$$\begin{aligned} x_{n+1} &= x_n + \delta x_n \left[r\left(1 - \frac{x_n}{K}\right) - \frac{a y_n}{(1+\alpha x_n)(1+\beta y_n)} \right] + u_n \\ y_{n+1} &= y_n + \delta y_n \left[\frac{b x_n}{(1+\alpha x_n)(1+\beta y_n)} - d \right] \end{aligned} \tag{17}$$

and

$$u_n = -k_1(x_n - x^*) - k_2(y_n - y^*)$$

where the feedback gains are denoted by $k_1$and k_2 and (x^*, y^*) represent positive fixed point of system (2).

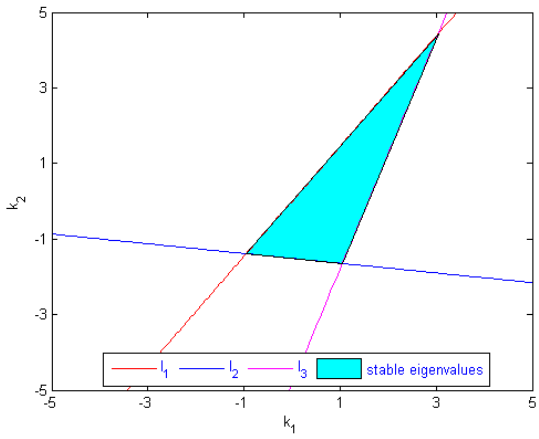

(a)

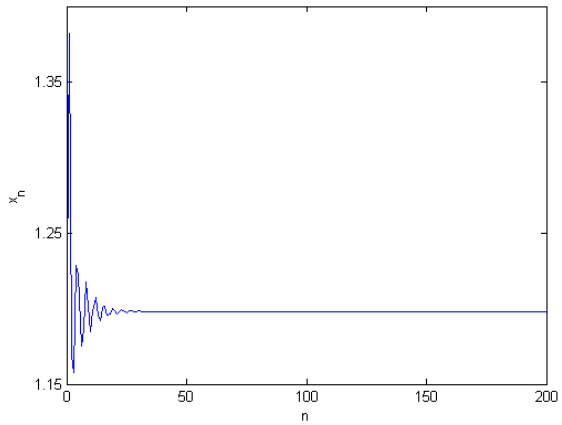

(b)

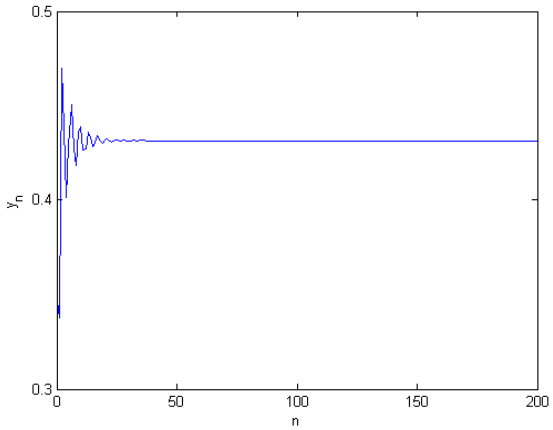

(c)

Fig. 9 Control of chaotic trajectories of system (17). (a) Stability region in (k_1, k_2) plane (b-c) Time series for states x and y respectively.

The Jacobian matrix J_c of the controlled system(17) is given by

$$J_c(x^*, y^*) = \begin{pmatrix} a_{11} - k_1 & a_{12} - k_2 \\ a_{21} & a_{22} \end{pmatrix} \tag{18}$$

where $a_{ij}, i, j = 1,2$ given in (7) are evaluated at (x^*, y^*). The characteristic equation of (18) is

$$\lambda^2 - (trJ_c)\lambda + detJ_c = 0 \tag{19}$$

where $trJ_c = a_{11} + a_{22} - k_1$ and $detJ_c = a_{22}(a_{11} - k_1) - a_{21}(a_{12} - k_2)$. Let λ_1 and λ_2 be the roots of (19). Then

$$\lambda_1 + \lambda_2 = a_{11} + a_{22} - k_1 \quad (20)$$

and

$$\lambda_1\lambda_2 = a_{22}(a_{11} - k_1) - a_{21}(a_{12} - k_2) \quad (21)$$

The solution of the equations $\lambda_1 = \pm 1$ and $\lambda_1\lambda_2 = 1$ determines the lines of marginal stability. These conditions confirm that $|\lambda_{1,2}| < 1$. Suppose that $\lambda_1\lambda_2 = 1$, then from (21) we have

$$l_1: a_{22}k_1 - a_{21}k_2 = a_{11}a_{22} - a_{12}a_{21} - 1.$$

Assume that $\lambda_1 = 1$, then from (20) and (21) we get

$$l_2: (1 - a_{22})k_1 + a_{21}k_2 = a_{11} + a_{22} - 1 - a_{11}a_{22} + a_{12}a_{21}.$$

Next, assume that $\lambda_1 = -1$, then from (20) and (21) we obtain

$$l_3: (1 + a_{22})k_1 - a_{21}k_2 = a_{11} + a_{22} + 1 + a_{11}a_{22} - a_{12}a_{21}.$$

Then the lines $l_1, l_2,$ and l_3 (see Fig. 9(a)) in the (k_1, k_2) plane determine a triangular region which keeps eigenvalues with magnitude less than 1.

In order to check how the implementation of feedback control method works and controls chaos at unstable state, we have performed numerical simulations. Parameter values are fixed as $\delta = 1.35$ and rest as in case (ii). The initial value is $(x_0, y_0) = (1.17, 0.35)$, and the feedback gains are $k_1 = 0.9$ and $k_2 = -0.08$. Figures 9(b) and 9(c) show that at the fixed point $(1.9809, 0.431542)$, the chaotic trajectory is stabilized.

6 Discussion

We investigate the dynamics of a discrete-time predator-prey system with Crowley-Martin functional response in the closed first quadrant $\mathbb{R}^2_+$. We prove via center manifold theorem and bifurcation theory, the system (2) can undergo a bifurcation (flip or NS) at unique positive fixed point if δ varies around the sets $FB^1_{E_2}$ or $FB^2_{E_2}$ and NSB_{E_2}. Numerical simulations present unpredictable behaviors of the system through a flip bifurcation which include orbits of period- 2, 4, 8 orbits and through a NS bifurcation which include an invariant cycle, orbits of period- 5, 6, 7, 10, 11, 15, 16, 17, 21, 28, and period- 51 orbits and chaotic sets respectively. These indicate that at the state of chaos, the system is unstable and particularly, the predator goes to extinct or goes to a stable fixed point when the dynamic of prey is chaotic. We confirm about the existence of chaos through the computation of maximum Lyapunov exponents and fractal dimension. Moreover, system (2) exhibits very rich nonlinear dynamical behaviors by the variation of two control parameters and one can directly observe the chaotic phenomenon from the two-dimensional parameter spaces. We observe that the increases values of control parameters α and β, can stabilize the dynamical system (2), but the small values may destabilize the system producing more complex dynamical behaviors. Finally, the chaotic trajectories at unstable state are controlled by implementing the strategy of feedback control. However, it is still a challenging problem to explore multiple parameter bifurcation in the system. We expect to obtain some more analytical results on this issue in the future.

References

Cartwright JHE. 1999. Nonlinear stiffness Lyapunov exponents and attractor dimension. Physics Letters A., 264: 298-304

Crowley PH, Martin EK. 1989. Functional responses and interference within and between year classes of a dragonfly population. Journal of the North American Benthological Society, 8: 211-221

Dong YY, Zhang SL, Li SB, Li YL. 2015. Qualitative analysis of a predator-prey model with Crowley-Martin functional response. International Journal of Bifurcation and Chaos, 25: 1550110

Elaydi SN. 1996. An Introduction to Difference Equations. Springer-Verlag, New York, USA

Elhassanein A. 2014. Complex dynamics of a stochastic discrete modified Leslie-Gower predator-prey model with Michaelis-Menten type prey harvesting. Computational Ecology and Software, 4(2): 116-28

Li SB, Wu JH, Dong YY. 2015. Uniqueness and stability of a predator-prey model with C-M functional response. Computers and Mathematics with Applications, 69: 1080-1095

He ZM, Lai X. 2011. Bifurcation and chaotic behavior of a discrete-time predator-prey system. Nonlinear Analysis: Real World Applications, 12: 403-417

He ZM, Li Bo. 2014. Complex dynamic behavior of a discrete-time predator-prey system of Holling-III type. Advances in Difference Equations, 180

Kaplan JL, Yorke YA. 1979. A regime observed in a fluid flow model of Lorenz, Communications in Mathematical Physics, 67: 93-108

Kuzenetsov YA. 1998. Elements of Applied Bifurcation Theory (2nd ed). Springer-Verlag, New York, USA

Nedorezov LV, Neklyudova. 2014. Continuous-discrete model of parasite-host system dynamics: Trigger regime at simplest assumptions. Computational Ecology and Software, 4(3): 163-169

Rana SMS. 2015a. Bifurcation and complex dynamics of a discrete-time predator-prey system. Computational Ecology and Software, 5(2): 187-200

Rana, SMS. 2015b. Bifurcation and complex dynamics of a discrete-time predator-prey system involving group defense. Computational Ecology and Software, 5(3): 222-238

Rana SMS. 2015c. Bifurcation and complex dynamics of a discrete-time predator-prey system with simplified Monod-Haldane functional response, Advances in Difference Equations, 345

Rana SMS. 2015d. Chaotic dynamics in a discrete-time predator-prey food chain. Computational Ecology and Software, 5(1): 28-47

Rana SMS, Kulsum U. 2017. Bifurcation analysis and chaos control in a discrete-time predator-prey system of Leslie type with simplified Holling Type IV functional response. Discrete Dynamics in Nature and Society, 2: 1-11

Rana SMS. 2017. Chaotic dynamics and control of discrete ratio-dependent predator-prey system. Discrete Dynamics in Nature and Society, 4537450

Rana SMS. 2019. Bifurcations and chaos control in a discrete-time predator-prey system of Leslie type. Journal of Applied Analysis and Computation, 9(1): 31-44

Ren J, Yu L, Siegmund S. 2017. Bifurcations and chaos in a discrete predator-prey model with Crowley-Martin functional response. Nonlinear Dynamics, 90(352)

Tripathi JP, Tyagi S, Abbas S. 2016. Global analysis of a delayed density dependent predator-prey model with Crowley-Martin functional response. Communications in Nonlinear Science and Numerical Simulation, 30: 45-69

Winggins S. 2003. Introduction to Applied Nonlinear Dynamical Systems and Chaos. Springer-Verlag, New York, USA

Zhang H, Ma S, Huang T, Cong X, Gao Z, Zhang F. 2018. Complex dynamics on the routes to chaos in a discrete predator-prey system with Crowley-Martin type functional response. Discrete Dynamics in Nature and Society, 2386954

Zhao M, Xuan Z, Li C. 2016. Dynamics of a discrete-time predator-prey system. Advances in Difference Equations, 191

Zhao M, Li C, Wang J. 2017. Complex dynamic behaviors of a discrete-time predator-prey system. Journal of Applied Analysis and Computation, 7: 478-500